Electrochemistry Communications 64 (2016) 26–29

Contents lists available at ScienceDirect

Electrochemistry Communications

journal homepage: www.elsevier.com/locate/elecom

Short communication

Tunable lithium storage properties of metal lithium titanates by stoichiometric modulation

Seongjun Bae [a,b,1], Young Geun Yoo [a,b,1], Inho Nam [a,b], Soomin Park [a,b], Jongseok Park [a,b], Jong Min Lee [a], Jeong Woo Han [c], Jongheop Yi [a,b,*]

[a] School of Chemical and Biological Engineering, Seoul National University, Seoul 151-742, Republic of Korea
[b] World Class University (WCU) Program of Chemical Convergence for Energy & Environment (C2E2), Institute of Chemical Processes, Seoul National University, Seoul 151-742, Republic of Korea
[c] Department of Chemical Engineering, University of Seoul, Seoul 130-743, Republic of Korea

ARTICLE INFO

Article history:
Received 9 January 2016
Accepted 15 January 2016
Available online 22 January 2016

Keywords:
Lithium-ion batteries
Potential control
Sodium strontium lithium titanate
Density functional theory

ABSTRACT

A simple stoichiometric modulation of $Na_{2-2x}Sr_xLi_2Ti_6O_{14}$ was developed to achieve tunable electrochemical properties of the material. The concept was confirmed experimentally and theoretically using density functional theory (DFT) calculations. Both the operating potential and the amount of reversibly intercalated lithium ions were manipulated by simply changing the Na/Sr ratio. These unique characteristics originated from a gradual change in the electron density on the Ti atoms and the extra lithium insertion sites at $SrLi_2Ti_6O_{14}$. As a promising anode material for lithium-ion batteries, $Na_{2-2x}Sr_xLi_2Ti_6O_{14}$ and its tunable electrochemical properties have significant importance in terms of the development of tailored electrodes with desirable electrochemical performance.

1. Introduction

Precise control of applied potential is an important technique during the operation of electronic devices (*e.g.*, OLEDs) due to its direct association with the overall efficiency [1,2]. However, battery systems cannot always satisfy the optimized potentials of every device because the output potential of batteries is always fixed. Therefore, the tunability of the operating potential of battery systems at the material level is highly desirable. However, strategies for adjusting the electrochemical properties of materials have rarely been reported due to the general assumption that the intrinsic property of these materials cannot be easily adjusted.

As a promising anode material for Li-ion batteries (LIBs), $MLi_2Ti_6O_{14}$ (MLTO, M = 2 Na, Sr, Ca, Ba and Pb) has been investigated with a focus on enhancement of its electrochemical performance for MLTOs containing single M species [3–11]. Previous studies have revealed that all of the MLTOs are constructed upon the same TiO_6 octahedral arrangements, which suggests the possibility of MLTO's preparation with two or more M species in the same material. Because the electrochemical properties of MLTO vary with the M species [12–16], MLTO with different electrochemical properties can be expected by merging two types of MLTOs.

The operating potential of titanate-based compounds is determined by the Ti^{3+}/Ti^{4+} redox energy [17]. The energy depends on the types of neighboring atoms and their relative positions with respective to Ti atom. Therefore, based on their species and stoichiometric combinations, M atoms can be employed to tune the MLTO operating potential. Moreover, an extra lithium insertion site is available in certain M species. Due to the characteristics of MLTOs, various operating potentials and gravimetric capacities can be achieved by controlling the stoichiometry of the M atoms.

Herein, we report the preparation of MLTOs with two co-existing M species for application as an anode material of LIBs. Utilizing the equivalent crystal structures of MLTOs, gradual modulation of the electrochemical properties is possible by controlling the M atom composition. To prove our concept, MLTO containing both sodium and strontium ($Na_{2-2x}Sr_xLi_2Ti_6O_{14}$, NaSrLTO) was employed, and the M species stoichiometry was controlled. The operating potential and equivalent amounts of reversibly intercalated lithium ions gradually changed as the Sr/Na ratio was modulated.

2. Experimental

$Na_{2-2x}Sr_xLi_2Ti_6O_{14}$ samples were prepared from $CH_3CO_2Na{\cdot}3H_2O$, $(CH_3CO_2)_2Sr{\cdot}0.5H_2O$, $CH_3CO_2Li{\cdot}2H_2O$, TiO_2 and oxalic acid (CH_3CO_2Na: $(CH_3CO_2)_2Sr$: CH_3CO_2Li: TiO_2: oxalic acid = $2-2x$: x: 2: 6: 2, x = 0, 0.25, 0.5, 0.75, 1). The powder was calcined in air at 1000 °C for 24 h to obtain the $Na_{2-2x}Sr_xLi_2Ti_6O_{14}$ samples that are 1–10 μm in size. Electrochemical measurements were carried out using CR2032-type coin cells at room temperature (25 °C). The electrodes were fabricated with the active material, Super P and poly(vinylidene difluoride) (PVdF) at a weight ratio of 8:1:1. These three components were mixed

* Corresponding author at: Seoul National University, School of Chemical and Biological Engineering, Seoul 151-742, Republic of Korea. Tel.: +82 2880 7438.
E-mail address: jyi@snu.ac.kr (J. Yi).
[1] These authors contributed equally to this work.

http://dx.doi.org/10.1016/j.elecom.2016.01.006
1388-2481/

with N-methylpyrrolidone (NMP) and cast on Cu foil using a doctor-blade with an active material mass loading of ≅1 mg/cm^2. The electrode was dried under vacuum at 120 °C for 12 h. A porous polypropylene film and 1.15 M $LiPF_6$ in an EC:EMC:DEC = 3:5:2 solvent were used for the separator and electrolyte, respectively. Galvanostatic charge/discharge tests were performed with a multichannel automatic battery cycler (WonATech, WBCS3000). DFT calculations using the Vienna *ab initio* simulation package code were employed to calculate the formation energies and Bader charge of Ti atoms in the crystal structure [18]. The details of the characterizations and DFT calculations have been described in a previous study [19].

3. Results and discussion

Fig. 1a shows the X-ray diffraction (XRD) patterns of NaSrLTOs. The patterns for $Na_2Li_2Ti_6O_{14}$ (NaLTO) and $SrLi_2Ti_6O_{14}$ (SrLTO) were in good agreement with those from previous studies on MLTOs [7,12,13]. These two samples exhibit similar patterns because NaLTO and SrLTO have analogous crystal structures. However, as shown in the magnified peak between 10° and 15°, the minor peaks corresponding to SrLTO gradually appeared with increasing Sr content. The difference in the minor peaks is due to the different stoichiometry of the Na and Sr atoms, where two Na atoms occupy an 11-fold-coordinated site and only one Sr atom occupies this site. These experimental XRD patterns are in good agreement with simulated results (Fig. 1b). Despite the minor differences in the lattice structure between NaLTO and SrLTO [12], NaSrLTOs form stable, well-crystallized structures.

DFT calculations were conducted to confirm the feasibility of NaSrLTO formation (Table 1). In general, the possibility of alloying two materials can be confirmed by comparing the formation energy of the mixed phases and pure phases. All of the mixed phases exhibited formation energies with negative values, which indicate that the Na, Sr-mixed phase is more stable than any of the separated phases. Due to the energetically stable structure of NaSrLTO, the synthesis of NaSrLTO with a single crystallinity is possible.

The electrochemical test results are shown in Fig. 2. Fig. 2a shows the galvanostatic charge/discharge profiles of NaSrLTOs in a potential window of 1.0–2.0 V. The amount of reversibly intercalated lithium ions was 2 Li equiv.$^{-1}$ with a potential plateau at 1.25 V for NaLTO and 2.5 Li equiv.$^{-1}$ at 1.4 V with an additional sloped plateau between 1.1 and 1.2 V for SrLTO. It is important to note that by increasing the Sr content in NaSrLTO, the working potential gradually shifted upward, and the amount of reversibly intercalated lithium ions increased linearly. Fig. 2b shows the rate capability test results. The samples with a higher Sr content exhibited better rate capability due to the higher electrical conductivity of SrLTO compared to that of NaLTO [12]. In long-term cycle tests at 200 mAh g^{-1}, all of the NaSrLTO samples exhibited a capacity retention in excess of 99% after 100 cycles (data are not shown).

Table 1
Calculated total energy and formation energy of $(1-x)Na_2Li_2Ti_6O_{14} + xSrLi_2Ti_6O_{14} \rightarrow Na_{2-2x}Sr_xLi_2Ti_6O_{14}$ (x = 0, 0.25, 0.5, 0.75, 1) based on the density functional theory (DFT) calculations.

	Total energy (eV)	Formation energy (ΔG, kJ mol^{-1})
$Na_2Li_2Ti_6O_{14}$	-1.21×10^3	0.00
$Na_{1.5}Sr_{0.25}Li_2Ti_6O_{14}$	-1.21×10^3	−16.2
$NaSr_{0.5}Li_2Ti_6O_{14}$	-1.19×10^3	−19.9
$Na_{0.5}Sr_{0.75}Li_2Ti_6O_{14}$	-1.15×10^3	−7.25
$SrLi_2Ti_6O_{14}$	-1.12×10^3	0.00

The differential capacity analyses of the charge curve at 10 mA g^{-1} demonstrated a shift in the potential plateau of NaSrLTOs (Fig. 2c). For NaLTO, an oxidation peak appeared at 1.27 V. However, the peaks for SrLTO were primarily located at 1.42 V and 1.15 V, which corresponds to two distinctive potential plateaus for SrLTO. The peak positions of NaSrLTOs are broader than those of NaLTO and SrLTO. The decrease in the sensitivity of the potential is due to distortion of the crystal structure derived from the different lattice constants of NaLTO and SrLTO. Nevertheless, the main oxidation peaks gradually shifted to a higher potential as the Sr content increased. In addition, the shoulder peak, which corresponds to the additional peak for SrLTO at 1.15 V, gradually faded as the content of Sr decreased.

The changes in the operating potential with NaSrLTOs originated from the atomic structure of MLTO. Fig. 3a shows the octahedral TiO_6 frameworks of NaSrLTOs, and the M atoms are located in the 8f Wyckoff positions. In NaLTO, the 8f Wyckoff position was fully occupied by two Na atoms, and this position in SrLTO was half occupied by one Sr atom. The similarity of the crystal structures of NaLTO and SrLTO results in substitution of 2 equivalent Na atoms to 1 equivalent Sr atom. By a gradual exchange of Na atoms with Sr atoms, the operating potential gradually increased from 1.25 V to 1.4 V due to the gradual change in the Ti^{3+}/Ti^{4+} redox reaction. Fig. 3b shows the differential charge density map near the Ti atoms. After the Na atoms were substituted by Sr atoms, the electron density near the Ti atoms decreased. Therefore,

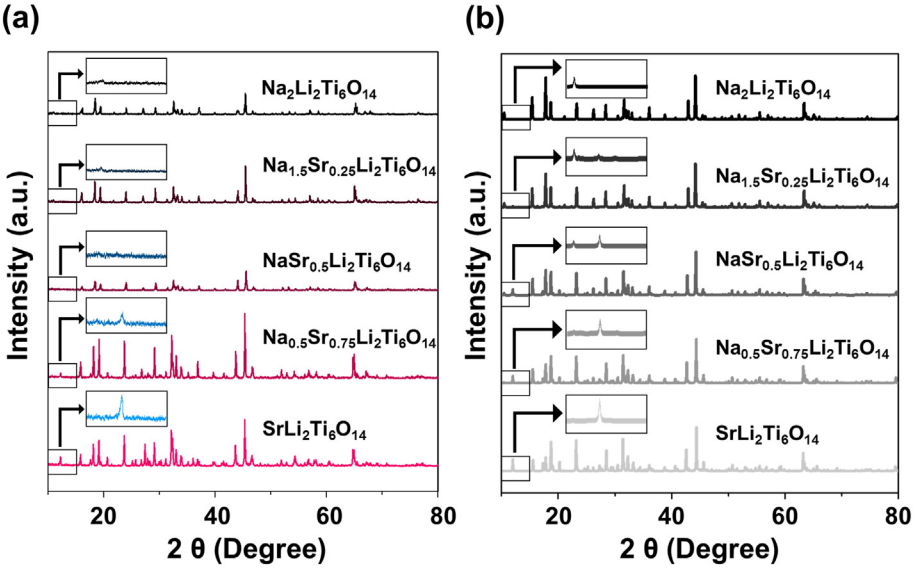

Fig. 1. XRD patterns of $Na_{2-2x}Sr_xLi_2Ti_6O_{14}$ from (a) experimental and (b) simulated data. The peaks in the magnified XRD patterns between 10° and 15° correspond to the (111) plane of $SrLi_2Ti_6O_{14}$.